Alfvén wave collisions, the fundamental building block of plasma turbulence. III. Theory for experimental design

G. G. Howes,[1,a)] K. D. Nielson,[1] D. J. Drake,[2] J. W. R. Schroeder,[1] F. Skiff,[1] C. A. Kletzing,[1] and T. A. Carter[3]
[1]*Department of Physics and Astronomy, University of Iowa, Iowa City, Iowa 52242, USA*
[2]*Department of Physics, Astronomy, and Geosciences, Valdosta State University, Valdosta, Georgia 31698, USA*
[3]*Department of Physics and Astronomy, University of California, Los Angeles, California 90095-1547, USA*

(Received 22 March 2013; accepted 11 June 2013; published online 15 July 2013)

Turbulence in space and astrophysical plasmas is governed by the nonlinear interactions between counterpropagating Alfvén waves. Here, we present the theoretical considerations behind the design of the first laboratory measurement of an Alfvén wave collision, the fundamental interaction underlying Alfvénic turbulence. By interacting a relatively large-amplitude, low-frequency Alfvén wave with a counterpropagating, smaller-amplitude, higher-frequency Alfvén wave, the experiment accomplishes the secular nonlinear transfer of energy to a propagating daughter Alfvén wave. The predicted properties of the nonlinearly generated daughter Alfvén wave are outlined, providing a suite of tests that can be used to confirm the successful measurement of the nonlinear interaction between counterpropagating Alfvén waves in the laboratory. © *2013 AIP Publishing LLC*. [http://dx.doi.org/10.1063/1.4812808]

I. INTRODUCTION

Turbulence is a ubiquitous phenomenon in space and astrophysical plasmas, driving a cascade of energy from large to small scales and strongly influencing the plasma heating resulting from the dissipation of the turbulence. Turbulence is believed to play a key role in a wide range of space and astrophysical plasma environments, influencing the heating of the solar corona and acceleration of the solar wind,[1] the dynamics of the interstellar medium,[2–4] the regulation of star formation,[5] the transport of heat in galaxy clusters,[6] and the transport of mass and energy into the Earth's magnetosphere.[7]

At the large length scales and low frequencies characteristic of the turbulence in astrophysical systems, the turbulent motions are governed by the physics of Alfvén waves.[8,9] In the idealized framework of incompressible magnetohydrodynamics (MHD), it has been shown that the turbulent cascade of energy from large to small scales is driven by the nonlinear interaction between counterpropagating Alfvén waves,[10] the key concept underpinning modern theories of Alfvénic turbulence.[11–13] This key concept remains at the foundation of theoretical investigations of astrophysical turbulence, yet its applicability in the moderately to weakly collisional conditions relevant to astrophysical plasmas has never been observationally or experimentally verified. Verification is necessary to establish a firm basis for the use of simplified fluid models, such as incompressible MHD, to examine the dynamics and consequences of turbulence in the weakly collisional conditions of diffuse astrophysical plasmas. In addition, the detailed nature of this nonlinear interaction forms the crucial distinction between the two leading theories for strong MHD turbulence.[12,13]

Several reasons make it unlikely that the nonlinear interaction between counterpropagating Alfvén waves can ever be verified using observations of turbulence in space or astrophysical environments. Remote astrophysical observations cannot achieve sufficient spatial resolution to identify individual Alfvénic fluctuations. *In situ* spacecraft measurements in the near-Earth solar wind are capable of sufficient resolution in time to identify the Alfvénic nature of fluctuations, but yield information at only a single spatial point (or a few spatial points for multi-spacecraft missions), insufficient to constrain the interaction between two counterpropagating Alfvénic fluctuations. Finally, in all of these systems, the broad spectrum of turbulent modes confounds attempts to identify the transfer of energy from two nonlinearly interacting Alfvén waves to a third wave. Only experimental measurements in the laboratory can achieve the controlled conditions and high spatial resolution necessary, but producing plasmas at the relevant magnetohydrodynamic scales requires a large experimental plasma volume. The unique capabilities of the Large Plasma Device (LAPD) at UCLA,[14] designed to study fundamental space plasma physics processes, make possible the first laboratory measurement of the nonlinear wave-wave interaction underlying Alfvénic turbulence.[15]

Howes and Nielson,[16] hereafter Paper I, presents the detailed derivation of an asymptotic analytical solution for the evolution of an Alfvén wave collision in the weakly nonlinear limit using the incompressible MHD equations. The fundamental insight into the nonlinear dynamics gleaned from this analytical solution lays the theoretical foundation for the experimental design described here. Nielson, Howes, and Dorland,[17] hereafter Paper II, presents a numerical verification of this analytical solution and demonstrates that the nonlinear interaction in a weakly collisional astrophysical plasma remains well described by the incompressible MHD

a)gregory-howes@uiowa.edu

solution. In this paper, we describe in detail the theoretical considerations used to design the first experiment to measure the nonlinear interaction between counterpropagating Alfvén waves.[15] A companion work by Drake *et al.*,[18] hereafter Paper IV, describes in detail the experimental setup and procedure and the analysis used to identify conclusively in the laboratory the nonlinear product of two counterpropagating Alfvén waves. Finally, in Howes *et al.*,[19] hereafter Paper V, the results of gyrokinetic numerical simulations of Alfvén wavepacket collisions are used to illustrate a magnetic shear interpretation of the nonlinear energy transfer occurring due to the counterpropagating Alfvén wave collision in the experiment designed here.

II. THEORY OF ALFVÉN WAVE COLLISIONS

Modern theories of anisotropic Alfvénic plasma turbulence, relevant to a wide range of space and astrophysical environments, have been developed largely based on several key concepts derived from the equations of incompressible MHD. Here, we review some fundamental properties of Alfvén wave collisions that provide the theoretical foundation for the design of an experiment to measure the nonlinear interaction between counterpropagating Alfvén waves in the laboratory.

A. Basic properties

As shown in Paper I, the equations of incompressible MHD can be written in a symmetrized Elsässer form,[20]

$$\frac{\partial \mathbf{z}^{\pm}}{\partial t} \mp \mathbf{v}_A \cdot \nabla \mathbf{z}^{\pm} = -\mathbf{z}^{\mp} \cdot \nabla \mathbf{z}^{\pm} - \nabla P/\rho_0, \tag{1}$$

$$\nabla^2 P/\rho_0 = -\nabla \cdot (\mathbf{z}^{-} \cdot \nabla \mathbf{z}^{+}), \tag{2}$$

where the magnetic field is decomposed into equilibrium and fluctuating parts $\mathbf{B} = \mathbf{B}_0 + \delta\mathbf{B}$, $\mathbf{v}_A = \mathbf{B}_0/\sqrt{4\pi\rho_0}$ is the Alfvén velocity due to the equilibrium field $\mathbf{B}_0 = B_0\hat{\mathbf{z}}$, P is total pressure (thermal plus magnetic), ρ_0 is mass density, and $\mathbf{z}^{\pm}(x,y,z,t) = \mathbf{u} \pm \delta\mathbf{B}/\sqrt{4\pi\rho_0}$ are the Elsässer fields given by the sum and difference of the velocity fluctuation $\mathbf{u}$ and the magnetic field fluctuation $\delta\mathbf{B}$ expressed in velocity units.

The symmetrized Elsässer form of the incompressible MHD equations lends itself to a particularly simple physical interpretation. The Elsässer field $\mathbf{z}^{+}$ represents either the Alfvén or pseudo-Alfvén wave traveling down the equilibrium magnetic field (in the anti-parallel direction), while $\mathbf{z}^{-}$ represents either one of these waves propagating up the equilibrium magnetic field (in the parallel direction). The second term on the left-hand side of Eq. (1) is the *linear term* representing the propagation of the Elsässer fields along the mean magnetic field at the Alfvén speed, the first term on the right-hand side is the *nonlinear term* representing the interaction between counterpropagating waves, and the second term on the right-hand side is a nonlinear term that ensures incompressibility through Eq. (2).

Paper I describes in detail the numerous linear and nonlinear properties of these equations, and here we highlight the principal properties that significantly influence the evolution of turbulence in an incompressible MHD plasma. First, it is shown that the Alfvén waves dominate the nonlinear dynamics of the turbulence[21] in the anisotropic limit, $k_\perp \gg k_\parallel$, a limit that naturally develops in magnetized plasma turbulence.[9,22–32] Second, the nonlinear interaction between two Alfvén waves occurs only when those Alfvén waves are propagating in opposite directions along the equilibrium magnetic field.[10,33] Third, the nonlinear interaction between two counterpropagating plane Alfvén waves with wavevectors $\mathbf{k}^{+}$ and $\mathbf{k}^{-}$ is proportional to $\hat{\mathbf{z}} \cdot (\mathbf{k}_\perp^{-} \times \mathbf{k}_\perp^{+})$, where perpendicular is defined with respect to the direction of the equilibrium magnetic field, $\mathbf{B}_0 = B_0\hat{\mathbf{z}}$. This implies that a nonzero nonlinear interaction between counterpropagating Alfvén waves requires that the two waves must have perpendicular components that are not collinear. Together, these properties dictate that the fundamental building block of turbulence in an incompressible MHD plasma is the nonlinear interaction between perpendicularly polarized, counterpropagating Alfvén waves.

B. Imbalanced wave amplitudes

Another property of Alfvén wave collisions that can be exploited in the design of an experiment to measure this nonlinear interaction involves using two counterpropagating Alfvén waves of different amplitudes. This property is apparent if we rewrite the equation for the evolution of the Elsässer field $\mathbf{z}^{+}$ in the following form:

$$\left[\frac{\partial}{\partial t} - \mathbf{v}_A \cdot \nabla\right] \mathbf{z}^{+} = -(\mathbf{z}^{-} \cdot \nabla)\mathbf{z}^{+} - \nabla P/\rho_0. \tag{3}$$

Noting that Eq. (2) shows that the pressure depends linearly on $\mathbf{z}^{+}$, the entire Eq. (3) is linear in $\mathbf{z}^{+}$. Ignoring the linear dependence on $\mathbf{z}^{+}$ that appears in every term of the equation, the terms on the right-hand side of Eq. (3), which are responsible for the nonlinear evolution of the $\mathbf{z}^{+}$ field, depend on the amplitude of the $\mathbf{z}^{-}$ field, but not on the amplitude of the $\mathbf{z}^{+}$ field. For example, for significantly different amplitudes $|\mathbf{z}^{+}| \ll |\mathbf{z}^{-}|$, the small-amplitude Alfvén wave corresponding to $\mathbf{z}^{+}$ will be strongly distorted nonlinearly by the large-amplitude $\mathbf{z}^{-}$ Alfvén wave, but the large-amplitude $\mathbf{z}^{-}$ Alfvén wave will only be weakly distorted by the small-amplitude $\mathbf{z}^{+}$ Alfvén wave. This interaction between waves of unequal amplitudes is related to the topic of imbalanced plasma turbulence (for the case of MHD turbulence, also referred to as turbulence with nonzero cross helicity).[34–38]

Therefore, to measure the nonlinear interaction between counterpropagating Alfvén waves, it is sufficient to produce only one large-amplitude *distorting* wave and to measure the nonlinear distortion of a small-amplitude *probe* wave. Note that the nonlinear distortion of the small amplitude probe wave, when its waveform is decomposed into Fourier modes, is represented by the transfer of energy into Fourier modes not present in the undistorted probe wave.

C. Weak MHD turbulence

For sufficiently small wave amplitudes, the nonlinear terms on the right-hand side of Eq. (1) are small compared to

the linear term, and one obtains a state of *weak MHD turbulence*.[11] In the weak turbulence paradigm, two counterpropagating Alfvén waves may interact nonlinearly to transfer energy to a third mode—this is the fundamental interaction that underlies the cascade of energy from large to small scales in a turbulent plasma. The small amplitude of the nonlinear term makes it possible to derive an analytical solution for the nonlinear evolution of weak MHD turbulence using perturbation theory.[16,39] It is important to note that the linear term in Eq. (1) has no counterpart in incompressible hydrodynamics, so it is not possible to define a state of weak incompressible hydrodynamic turbulence. Incompressible hydrodynamic turbulence is always strong, precluding the application of perturbation theory to obtain an analytical solution. This is an important, and often underappreciated, fundamental distinction between the turbulence in incompressible hydrodynamic systems and that in incompressible MHD systems.

Applying perturbation theory to the case of two counterpropagating plane Alfvén waves with wavevectors $\mathbf{k}_1$ and $\mathbf{k}_2$, the lowest-order nonlinear interaction is the three-wave interaction with a third mode with wavevector $\mathbf{k}_3$. When averaged over an integral number of wave periods, this three-wave interaction satisfies the resonance conditions

$$\mathbf{k}_1 + \mathbf{k}_2 = \mathbf{k}_3 \quad \text{and} \quad \omega_1 + \omega_2 = \omega_3. \tag{4}$$

These constraints are equivalent to the conservation of momentum and conservation of energy.[11,39]

During the late 1990s, significant controversy arose regarding the nature of weak MHD turbulence, focused on the question of whether the lowest-order, nonzero nonlinear interactions are three-wave or four-wave interactions. The history of this controversy is thoroughly outlined in Paper I, but here we briefly discuss a few relevant details because our aim is to design an experiment that leads to a nonzero three-wave interaction.

Consider the nonlinear interaction between two counterpropagating plane Alfvén waves with wavevectors $\mathbf{k}_1$ and $\mathbf{k}_2$. The linear dispersion relation gives the Alfvén wave frequency in terms of the component of the wavevector parallel to the equilibrium magnetic field, $\omega = |k_\parallel| v_A$. Here, we adopt the convention that the frequency is always positive, $\omega > 0$, so that the sign of $k_\parallel$ indicates the direction of propagation of the wave along the equilibrium magnetic field. As discussed earlier, a nonzero nonlinearity requires counterpropagating Alfvén waves, implying that $k_{\parallel 1}$ and $k_{\parallel 2}$ have opposite signs. It has been pointed out that the only nontrivial solution to both constraints in Eq. (4) therefore has either $k_{\parallel 1} = 0$ or $k_{\parallel 2} = 0$.[25] The consequence of this finding is that there is no cascade of energy to higher parallel wavenumber in weak MHD turbulence. Further, since propagating plane Alfvén waves require nonzero $k_\parallel$, this led early researchers to posit that the three-wave interaction in weak MHD turbulence—the lowest order in the perturbative expansion—was zero, and that the four-wave interaction represented the lowest-order, nonzero nonlinear interaction.[11] The hypothesis that three-wave interactions were empty was later demonstrated to be false because, in a turbulent astrophysical system, the tendency for adjacent magnetic field lines to wander away from each other manifests itself as an effective $k_\parallel = 0$ component to the turbulence.[39–41] Therefore, the leading order of turbulent energy transfer in a weakly turbulent MHD plasma obeys the constraints imposed in Eq. (4) and no parallel cascade of energy occurs.

D. Weakly nonlinear Alfvén wave collisions

In the design of a laboratory experiment to measure an Alfvén wave collision, the importance of whether the lowest-order nonlinear interaction between counterpropagating Alfvén waves is a three-wave or four-wave interaction cannot be overstated. Consider the interaction between two counterpropagating Alfvén waves, each with amplitude δB, in a magnetized plasma with an equilibrium magnetic field of magnitude B_0. The amplitude[11,40] of a mode generated by three-wave interactions is proportional to $(\delta B/B_0)^2$, whereas the amplitude of a mode generated by four-wave interactions is proportional to $(\delta B/B_0)^3$. Since achievable wave amplitudes in the laboratory are typically small compared to the equilibrium magnetic field, $\delta B/B_0 \ll 1$, the signal due to a four-wave interaction will be significantly smaller than that arising from a three-wave interaction.

In order to develop valuable physical intuition about the nature of Alfvén wave collisions, in Paper I we derived an asymptotic analytical solution for the nonlinear interaction between counterpropagating Alfvén waves in the weakly nonlinear limit. Here, we briefly outline the properties of that solution and use the resulting insight to identify the necessary aspects of the experimental design to achieve a nonzero three-wave nonlinear interaction in the laboratory. A more detailed qualitative description of this analytical solution is provided in Sec. IV A of Paper I.

The asymptotic solution employs the incompressible MHD equations to solve for the evolution of the nonlinear interaction between two counterpropagating plane Alfvén waves, with wavevectors $\mathbf{k}_1^+ = k_{\perp 0}\hat{\mathbf{x}} - k_{\parallel 0}\hat{\mathbf{z}}$ and $\mathbf{k}_1^- = k_{\perp 0}\hat{\mathbf{y}} + k_{\parallel 0}\hat{\mathbf{z}}$, where the equilibrium magnetic field is $\mathbf{B}_0 = B_0\hat{\mathbf{z}}$. The plasma inhabits a periodic domain of size $L_\parallel \times L_\perp^2$ that is elongated along the direction of the equilibrium magnetic field such that $L_\parallel \gg L_\perp$. The wavenumber components of the initial Alfvén waves are at the domain scale, $k_{\perp 0} \equiv 2\pi/L_\perp$ and $k_{\parallel 0} \equiv 2\pi/L_\parallel$, so that problem models the nonlinear dynamics in the *anisotropic limit*, $k_\perp \gg k_\parallel$. In this limit, the Alfvénic dynamics decouples from the dynamics of the pseudo-Alfvén waves, and the nonlinear evolution of the Alfvénic fluctuations is rigorously described by the Elsässer potential equations.[21] The characteristics of the nonlinear solution outlined below are described using a shorthand notation for the spatial Fourier modes, $(k_x/k_{\perp 0}, k_y/k_{\perp 0}, k_z/k_{\parallel 0})$, such that the initial Alfvén waves are denoted by $\mathbf{k}_1^+ = (1, 0, -1)$ and $\mathbf{k}_1^- = (0, 1, 1)$.

The lowest-order nonlinear solution arises from a three-wave interaction in which the primary Alfvén waves $\mathbf{k}_1^+$ and $\mathbf{k}_1^-$ interact to transfer energy to a secondary mode $\mathbf{k}_2^{(0)} = (1, 1, 0)$. This mode is a strictly magnetic fluctuation with no variation along the equilibrium magnetic field, $k_\parallel = 0$, but with an oscillation frequency $2\omega_0$. Since this

mode does not satisfy the linear Alfvén wave dispersion relation, it is an inherently nonlinear fluctuation. In addition, the nonlinear interaction between $\mathbf{k}_1^+$ and $\mathbf{k}_1^-$ also generates an electromagnetic standing wave caused by the superposition of two counterpropagating linear Alfvén waves with wavevectors $\mathbf{k}_2^{(-2)} = (-1, 1, 2)$ and $\mathbf{k}_2^{(+2)} = (1, -1, -2)$, each with frequency $2\omega_0$. The amplitude of all three of these Fourier modes, each generated by nonlinear three-wave interactions, oscillates in time as shown by Eqs. (5)–(8) in Paper II, so there is no secular transfer of energy for the lowest-order nonlinear solution.

Since the interacting primary Alfvén waves have no $k_\parallel = 0$ component, there is no net energy transfer for the lowest-order nonlinear solution (resulting from three-wave interactions), consistent with the findings of Ng and Bhattacharjee.[40] Physically, since the equilibrium magnetic field defined in our periodic domain does not wander—the relevant situation for a laboratory plasma experiment confined by a uniform, axial magnetic field—the three-wave interaction leads to zero net transfer of energy at any time equal to a half-integral number of primary wave periods, $t = n\pi/\omega_0$ for $n = 1, 2, 3, \ldots$. This case contrasts with the argument for turbulent astrophysical plasmas, described in Sec. II C, in which field-line wander leads to an effective $k_\parallel = 0$ component to the turbulence, enabling a net transfer of energy due to three-wave interactions.

The secular transfer of energy first arises in this problem due to four-wave interactions appearing at the next order of the asymptotic solution in Paper I. When the secondary mode $\mathbf{k}_2^{(0)}$ has nonzero amplitude, the two primary Alfvén waves $\mathbf{k}_1^+$ and $\mathbf{k}_1^-$ nonlinearly interact with it to transfer energy to two tertiary Alfvén waves $\mathbf{k}_3^+ = (2, 1, -1)$ and $\mathbf{k}_3^- = (1, 2, 1)$, respectively. The amplitudes of these tertiary Alfvén waves increase linearly with time, indicating a secular transfer of energy. The net effect of combining these two three-wave interactions—the interaction $\mathbf{k}_1^+ + \mathbf{k}_1^- = \mathbf{k}_2^{(0)}$ followed by $\mathbf{k}_1^\pm + \mathbf{k}_2^{(0)} = \mathbf{k}_3^\pm$—is equivalent to a four-wave interaction that causes the secular transfer of energy from the primary Alfvén waves at low wavenumber with $|\mathbf{k}_1^\pm| = \sqrt{k_{\perp 0}^2 + k_{\parallel 0}^2}$ to the tertiary Alfvén waves at higher wavenumber with $|\mathbf{k}_3^\pm| = \sqrt{5k_{\perp 0}^2 + k_{\parallel 0}^2}$. In agreement with the heuristic model of weak turbulence,[11,39,41–43] this nonlinear energy transfer is strictly perpendicular, manifesting a perpendicular cascade of energy to higher $k_\perp$, but no parallel cascade of energy to higher $k_\parallel$.

E. Implications for experimental design

Exploiting the physical insight derived from the theoretical considerations outlined above in this section, we discuss here the characteristics of the experiment necessary to achieve a measurable nonlinear interaction between counterpropagating Alfvén waves in the laboratory.

The experiment[15] was performed using the Large Plasma Device (LAPD),[14] a basic plasma science user facility operated at the University of California, Los Angeles. This experimental apparatus generates a plasma in a cylindrical column of 16.5 m length and 40 cm diameter confined by a background axial magnetic field. The basic setup is to employ two separate antennas, located at opposite ends of the plasma chamber, to launch Alfvén waves in opposite directions along the equilibrium axial magnetic field. The wave magnetic fields of the two linearly polarized Alfvén waves are oriented perpendicular to each other to maximize the nonlinear interaction, satisfying the desired properties outlined in Sec. II A.

The two antennas used for the experiment, a Loop antenna[44] and an Arbitrary Spatial Waveform (ASW) antenna,[45,46] have different capabilities that can be exploited to optimize the resulting nonlinear signal in the experiment. The Loop antenna can generate a relatively large-amplitude Alfvén wave (up to $\delta B/B_0 \sim 0.01$, although in this experiment we use $\delta B/B_0 \sim 0.002$), but the spatial waveform in the plane perpendicular to the axial magnetic field consists of a complicated combination of Fourier modes, making the identification of any nonlinear distortion of this wave difficult. The ASW antenna, on the other hand, can generate a spatial waveform dominated by a single plane-wave Fourier mode, simplifying the task of measuring the nonlinear energy transfer to a different Fourier component, but is limited to much smaller Alfvén wave amplitudes ($\delta B/B_0 \sim 0.00002$). Therefore, we choose to perform the experiment with counterpropagating Alfvén waves of unequal amplitude, using a large-amplitude *distorting* Alfvén wave launched by the Loop antenna to cause nonlinear evolution of a small-amplitude *probe* Alfvén wave launched by the ASW antenna, taking advantage of the properties of the nonlinear interaction discussed in Sec. II B.

The instrumental limitation to small Alfvén wave amplitudes compared to the equilibrium magnetic field, $\delta B/B_0 \ll 1$, leads to a system with dynamics that satisfy the weakly nonlinear limit. In addition, the plasma volume in the experiment is highly elongated along the equilibrium magnetic field, leading to nonlinear dynamics within the anisotropic limit, $k_\perp \gg k_\parallel$. Finally, the strong equilibrium magnetic field in the experiment is usually chosen to be as straight and uniform as possible to yield good plasma confinement, so the equilibrium magnetic field lines do not wander, in contrast to the astrophysical case. Fortunately, these experimental limitations lead to a system that is directly comparable to the asymptotic analytical solution outlined in Sec. II D, so we can use this solution to guide the experimental design.

Our goal is to devise an experiment that will generate a propagating *daughter* Alfvén wave due to a secular transfer of energy from the primary interacting Alfvén waves. It is important that this nonlinearly generated daughter Alfvén wave has a sufficient amplitude to be measurable in the laboratory, even in the weakly nonlinear limit dictated by instrumental limitations. Therefore, it is desirable that this energy transfer be governed by a three-wave interaction, which produces a significantly larger amplitude signal than a four-wave interaction. However, for the symmetric Alfvén wave collision problem defined in Sec. II D, in which the two primary Alfvén waves have equal and opposite values of $k_\parallel$, the

three-wave interaction between these primary Alfvén waves does not yield a secular transfer of energy. The four-wave interaction, on the other hand, does lead to a net secular transfer of energy to a propagating daughter Alfvén wave. This four-wave interaction consists of the sequence of three-wave interactions $\mathbf{k}_1^+ + \mathbf{k}_1^- = \mathbf{k}_2^{(0)}$ followed by $\mathbf{k}_1^\pm + \mathbf{k}_2^{(0)} = \mathbf{k}_3^\pm$, where the nonlinearly generated magnetic fluctuation with $k_\parallel = 0$ plays a key role in mediating the energy transfer. However, the amplitude of the daughter Alfvén wave generated nonlinearly by this four-wave interaction is unlikely to have a sufficient signal-to-noise ratio to be measurable in the laboratory.

Upon examination of the two sequential three-wave interactions constituting the four-wave interaction in the symmetric problem, the second of these interactions, $\mathbf{k}_1^\pm + \mathbf{k}_2^{(0)} = \mathbf{k}_3^\pm$, has the property we desire: the nonlinear transfer of energy from one propagating Alfvén wave $\mathbf{k}_1^\pm$ to another propagating Alfvén wave $\mathbf{k}_3^\pm$ with higher perpendicular wavenumber. Therefore, we require that the waveform of one of the propagating Alfvén waves, in this case the large-amplitude distorting Alfvén wave, include a $k_\parallel = 0$ component. This will satisfy the requirement, discussed in Sec. II C, that one of the interacting modes in the three-wave interaction has $k_\parallel = 0$. This property can be achieved in the laboratory by breaking the symmetry between the parallel wavenumbers of the two primary counterpropagating Alfvén waves.

In our approach, the Loop antenna launches a large-amplitude distorting Alfvén wave $\mathbf{z}^-$ up the axial magnetic field. This distorting Alfvén wave has a longer parallel wavelength, $\lambda_\parallel^- = 2\pi/k_\parallel^-$, than the parallel wavelength, $\lambda_\parallel^+$, of the counterpropagating, small-amplitude probe Alfvén wave $\mathbf{z}^+$ launched by the ASW antenna, such that $\lambda_\parallel^- > \lambda_\parallel^+$. Furthermore, the distorting antenna parallel wavelength is longer than twice the physical distance L over which the two counterpropagating waves interact, $\lambda_\parallel^- > 2L$. As demonstrated quantitatively in Sec. III, for this case, the section of the waveform of the distorting Alfvén wave that interacts with the probe Alfvén wave will, in general, have a nonzero $k_\parallel = 0$ component. Therefore, the distorting Alfvén wave can mediate the secular transfer of energy from the primary probe Alfvén wave, through a nonlinear three-wave interaction, to a propagating daughter Alfvén wave. The resulting nonlinear evolution is consistent with the findings of Ng and Bhattacharjee[40] that nonlinear energy transfer due to three-wave interactions is nonzero when the interacting wavepackets have a $k_\parallel = 0$ component. In Sec. II F below, we discuss in more detail the physical significance of an Alfvén wavepacket with a $k_\parallel = 0$ component.

Note that, experimentally, the parallel wavelength of an Alfvén wave launched by an antenna in the LAPD is controlled by the driving frequency of the antenna. The argument above can be cast into a complementary form using the temporal basis of period or frequency instead of wavelength or wavenumber. For Alfvén waves in the MHD limit, which are non-dispersive, the linear dispersion relation connecting these alternative descriptions is simply $\lambda_\parallel = v_A T$. The equivalent temporal description is that we use a low-frequency distorting Alfvén wave to nonlinearly modify a counterpropagating higher-frequency probe Alfvén wave. The time over which the two waves interact is less than the period of the low-frequency distorting Alfvén wave, leading to a nonzero net energy transfer mediated by a three-wave interaction. Note that all of the Alfvén wave frequencies used in the experiment must be somewhat below the ion cyclotron frequency, typically $\omega \lesssim \Omega_i/2$, to prevent the cyclotron resonance from significantly altering the Alfvén wave dynamics.[47]

F. Plane waves versus wavepackets

The controversy over the existence of three-wave interactions in weak MHD turbulence arose partly through the consideration of a problem that was implicitly restricted to the interactions between plane Alfvén waves, where each plane wave mode is described by its single wavevector, $\mathbf{k}$. For a plane Alfvén wave to propagate, the parallel component of this wavevector must be nonzero. The physical reason is that magnetic tension is the restoring force that supports the propagation of Alfvén waves, and only modes with $k_\parallel \neq 0$ bend the equilibrium magnetic field. If one has a single spatial Fourier mode with $k_\parallel = 0$, the magnetic field is not bent, so there arises no magnetic tension to support Alfvén wave propagation.

But a more physically relevant case to consider than the interaction between two plane Alfvén waves of infinite extent is the interaction between two spatially localized Alfvén wavepackets.[40] This more general case of wavepacket interactions leads to a significantly different perspective on the role of $k_\parallel = 0$ modes, as follows. First, as shown in Paper I, we note that, in the absence of any Alfvén wave energy propagating in the opposite direction ($\mathbf{z}^+ = 0$), a finite amplitude Alfvén wave $\mathbf{z}^-$ of arbitrary waveform is an exact nonlinear solution to 1. Any such Alfvén wavepacket $\mathbf{z}^-$ will propagate undistorted up the equilibrium magnetic field at the Alfvén speed, v_A. Next, for an incompressible MHD plasma with an equilibrium magnetic field $\mathbf{B}_0 = B_0\hat{\mathbf{z}}$, we consider the two different waveforms of Alfvén wavepackets presented in Figure 1. The waveform in panel (a) is symmetric about $\delta B_x = 0$, so a Fourier decomposition of this wavepacket has no $k_\parallel = 0$ component. The waveform in panel (b), on the other hand, is not symmetric about $\delta B_x = 0$,

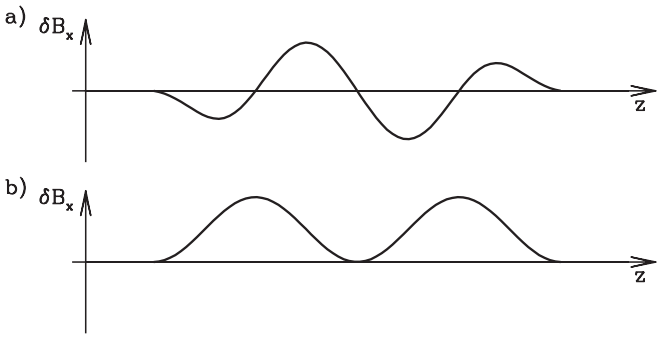

FIG. 1. Schematic diagram of the waveforms of two Alfvén wavepackets. (a) A waveform that is symmetric about $\delta B_x = 0$, and that therefore has no $k_\parallel = 0$ component. (b) An asymmetric waveform that includes a significant $k_\parallel = 0$ component.

and therefore a Fourier decomposition yields a significant $k_\parallel = 0$ component to this Alfvén wavepacket. Yet, in the absence of any counterpropagating Alfvén wavepackets, $\mathbf{z}^+ = 0$, both of these Alfvén wavepackets will propagate similarly up the equilibrium magnetic field at the Alfvén speed without any nonlinear distortion, even for finite wave amplitude.

When a counterpropagating Alfvén wavepacket $\mathbf{z}^+$ with no $k_\parallel = 0$ component collides with one of the waveforms in Figure 1, however, the nonlinear evolution differs significantly for these two cases. For the case involving the symmetric waveform in panel (a), there will be no three-wave interaction since neither wavepacket has a $k_\parallel = 0$ component. The lowest-order nonlinear interaction in this case is the four-wave interaction.[11] For the case involving the asymmetric waveform in panel (b), however, the $k_\parallel = 0$ component of the $\mathbf{z}^-$ wavepacket leads to a three-wave interaction that nonlinearly distorts the counterpropagating $\mathbf{z}^+$ Alfvén wavepacket.

In a turbulent astrophysical plasma, of course, there is no reason that the many Alfvén wavepackets that constitute the turbulence need have symmetric waveforms. In general, one would expect the waveform of any given Alfvén wavepacket not to be symmetric, so it is therefore expected that three-wave interactions will dominate in the case of weak turbulence in an astrophysical plasma.[40] In Paper V, we show that the $k_\parallel = 0$ component of an Alfvén wavepacket is equivalent to a magnetic shear, establishing the connection between magnetic field line wander and plasma turbulence.

The key point to take away from this discussion is that an asymmetric Alfvén waveform will generate a three-wave interaction because its plane wave decomposition contains a finite $k_\parallel = 0$ component. In the laboratory, we aim to design an experiment that will generate such an asymmetric Alfvén waveform, and will therefore lead to nonlinear energy transfer through a three-wave interaction. In the next section, we demonstrate quantitatively that, for the particular experimental setup chosen, the waveform of the large-amplitude distorting Alfvén wave includes the desired $k_\parallel = 0$ component.

III. EXPERIMENTAL DESIGN

The aim of this paper is to explain the theoretical considerations underlying the design of an experiment to measure the product of the nonlinear interaction between perpendicularly polarized, counterpropagating Alfvén waves in the laboratory. The experiment is designed to measure the interaction between a large-amplitude, low-frequency *distorting* Alfvén wave and a counterpropagating smaller-amplitude, higher-frequency *probe* Alfvén wave. In this section, we demonstrate that the nonlinear interaction in this experimental setup will generate a propagating Alfvén wave from the lowest-order, three-wave interaction, and we predict the properties of this nonlinear *daughter* Alfvén wave.

A simplified schematic of the LAPD experiment is shown in Figure 2. The Loop antenna[44] generates a relatively large-amplitude, distorting Alfvén wave $\mathbf{z}^-$, with its wave magnetic field dominantly polarized in the x-direction, traveling up the equilibrium axial magnetic field, $\mathbf{B}_0 = B_0\hat{\mathbf{z}}$. The

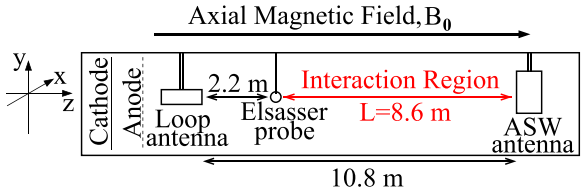

FIG. 2. Schematic of the Alfvén wave turbulence experiment on the LAPD. The Loop antenna generates a large-amplitude distorting Alfvén wave, with the wave magnetic field dominantly polarized in the x-direction, traveling up the equilibrium axial magnetic field, $\mathbf{B}_0 = B_0\hat{\mathbf{z}}$. The ASW antenna generates a small-amplitude probe Alfvén wave polarized in the y-direction traveling down the axial magnetic field.

Arbitrary Spatial Waveform (ASW) antenna[45,46] generates a small-amplitude, probe Alfvén wave $\mathbf{z}^+$, polarized in the y-direction, traveling down the axial magnetic field. The magnetic and electric field signals of the waves are measured by an Elsässer probe[48] located near the Loop antenna. The probe Alfvén wave is nonlinearly distorted by the counterpropagating Loop Alfvén wave over the length of the *interaction region* between the ASW antenna and the Elsässer probe, $L = 8.6$ m, as depicted in Figure 2.

If the parallel wavelength of the distorting Alfvén wave $\lambda_\parallel^- > 2L$, then the probe Alfvén wave will interact with only a fraction of a wavelength of the distorting wave before it is measured by the Elsässer probe. In this case, the net effect of the three-wave interaction is nonzero because the distorting wave effectively includes a $k_\parallel = 0$ component. The experiment described here, and in our companion work Paper IV,[18] is aimed at measuring the nonlinear outcome of that interaction in the laboratory.

A. The waveform of the distorting wave over the interaction region

For a sufficiently long parallel wavelength of the distorting Alfvén wave $\mathbf{z}^-$ such that $\lambda_\parallel^- > 2L$, each point on the counterpropagating probe Alfvén wave $\mathbf{z}^+$ interacts with only a fraction of the waveform before it is measured by the Elsässer probe. To demonstrate this quantitatively, it is instructive to illustrate this interaction as a function of time, as depicted in Figure 3. All of the parameters of the LAPD experiment are provided in Paper IV,[18] so here we merely quote the values of the parameters relevant to this discussion. The parallel wavelength of the distorting Loop Alfvén wave is $\lambda_\parallel^- = 29.1$ m and of the probe ASW Alfvén wave is $\lambda_\parallel^+ = 6.4$ m. The interaction region spans $L = 8.6$ m along the equilibrium magnetic field between the ASW antenna and the Elsässer probe, as shown in Figure 2.

In Figure 3, the distorting Loop Alfvén wave travels to the right at the Alfvén velocity v_A in the upper plot of each panel (the Loop antenna is physically located just to the left of the ordinate axis). Similarly, the lower plot of each panel shows the probe Alfvén wave traveling to the left at the Alfvén velocity v_A, launched from the ASW antenna (center, vertical dotted line) towards the Elsasser probe (left, vertical long-dashed line). Note that the length L on the left side, between the Elsasser probe and the ASW antenna, corresponds to the interaction region in the experiment. The length L to the right of the ASW antenna is included to show

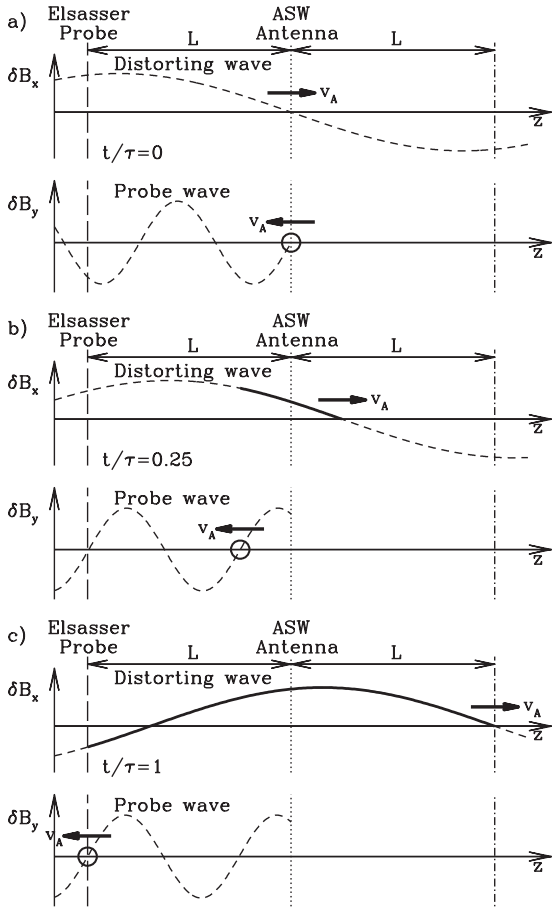

FIG. 3. Each panel depicts the δB_x component of the rightward propagating distorting Loop Alfvén wave (upper) and the δB_y component of the leftward propagating probe ASW Alfvén wave (lower). The length of the distorting Alfvén wave that has interacted with one point on the probe Alfvén wave (open circle) is depicted by the thick solid line in the upper plot of each panel.

the part of the distorting Alfvén wave that has passed the position of the ASW antenna (physically, this part of the wave is disrupted by the presence of the ASW antenna).

Let us consider the length of the distorting Alfvén wave that has interacted with a particular point on the probe Alfvén wave (marked by an open circle in the lower plot of each panel in Figure 3). We plot the length of the distorting Alfvén wave that has interacted (thick solid line) as a function of time normalized by $\tau = v_A/L$, the probe wave travel time from the ASW antenna (center, vertical dotted line) to the Elsässer probe (left, vertical long-dashed line). In panel (a), at $t/\tau = 0$, the point on the probe wave is just leaving the ASW antenna (lower), and has not interacted with any of the distorting wave (upper). In panel (b), at $t/\tau = 0.25$, the particular point on the probe wave (open circle) has moved one quarter of the distance from the ASW antenna to the Elsässer probe (lower). The section of the distorting wave that has interacted with the particular point of the probe wave (upper) is indicated by the thick solid line. Note that this section of thick solid line is twice the distance that the probe Alfvén wave has traveled since the relative speed between the two counterpropagating waves is $2v_A$. In panel (c), at $t/\tau = 1$, the point on the probe wave has reached the Elsässer probe where it is measured (lower). That point on the probe wave has interacted with the portion of the distorting wave (upper) that spans a length $2L$ (thick solid line).

The plots in Figure 3 illustrate that the nonlinear interaction is the result of a length $2L$ of the distorting wave interacting with each point on the probe wave. The key concept here is that, as long as $\lambda_\parallel^- > 2L$, the probe wave interacts with only a fraction of the wavelength of the distorting wave. Even though an integral number of wavelengths of the distorting wave has no $k_\parallel = 0$ component, the waveform over a length that is a non-integral number of wavelengths contains a $k_\parallel = 0$ component. The resulting waveform of the distorting Alfvén wave that is responsible for nonlinearly modifying the probe wave is indicated by the thick solid line in the upper plot of panel (c). In Sec. III B, we show that this part of the distorting Alfvén wave contains an effective $k_\parallel = 0$ component.

B. Fourier components of the distorting wave

To understand how the experimental design we have chosen is able to generate nonlinearly a propagating daughter Alfvén from the lowest-order, three-wave interaction, we must consider the section of the distorting Loop Alfvén wave, as depicted by the thick solid line in the upper plot of panel (c) in Figure 3, which is responsible for causing a nonlinear distortion of the probe Alfvén wave. We can Fourier transform to decompose that waveform into its plane wave components, and consider the nonlinear interaction of each of those components of the distorting wave with the probe wave.

The Fourier decomposition of the distorting Alfvén wave is shown in Figure 4. In panel (a) is shown the full waveform of the distorting Alfvén wave, the same waveform as that given by the thick solid line in the upper part of panel (c) in Figure 3. The parallel length of the signal is $2L$, so the components of the Fourier transform have parallel wavenumbers $k_\parallel = 0, \pi/L, 2\pi/L, 3\pi/L, \ldots$, and the lowest five Fourier modes are plotted in panels (b)–(f).

Figure 4 makes clear the key point that, although the distorting Loop Alfvén wave is simply a single sinusoidal component with wavelength $\lambda_\parallel^- = 29.1\,\mathrm{m}$, when sampled over only a fraction of its wavelength, it can have a significant $k_\parallel = 0$ component that interacts with the counterpropagating probe ASW Alfvén wave. This effective $k_\parallel = 0$ component, shown in panel (b), is in fact the energetically dominant component for the particular case examined in Figure 4. The $k_\parallel = \pi/L$ mode also contains significant energy, but the higher-order components with $k_\parallel > \pi/L$ contain very little energy. Therefore, for the particular case examined here, the dominant components of the distorting Alfvén wave that interact with the probe Alfvén wave are the two lowest wavenumber components of the Fourier series, $k_\parallel = 0$ and $k_\parallel = \pi/L$.

It is worthwhile pointing out that the results of the Fourier decomposition shown in Figure 4 depend on the what section (of length $2L$) of the distorting Alfvén wave is sampled. As a window of length $2L$ is moved over the Loop antenna waveform, which has a parallel wavelength $\lambda_\parallel^- = 29.1\,\mathrm{m}$, the coefficient of the $k_\parallel = 0$ Fourier component

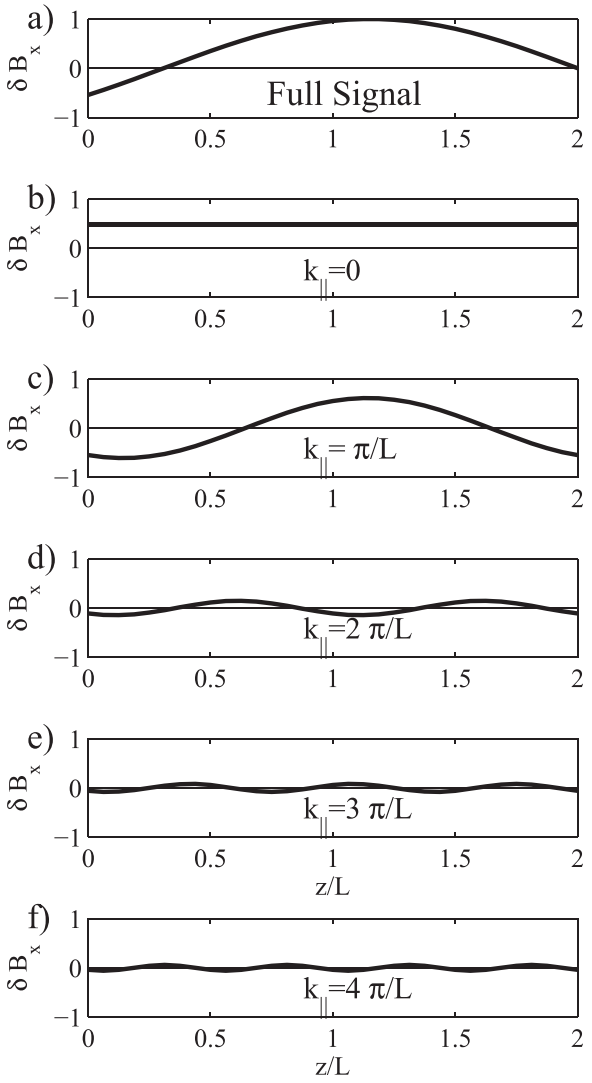

FIG. 4. Fourier decomposition of the distorting Alfvén wave signal over a length $2L$, showing that the waveform contains a significant $k_\parallel = 0$ component.

oscillates about zero. This coefficient reaches an extremum when the window is centered on an extremum of the distorting Loop antenna wave (so that the windowed signal has even parity about the center), and passes through zero when the window is centered on a zero crossing of the distorting Loop antenna wave (so that the windowed signal has odd parity). As we shall see, this property implies that the measured amplitude of the nonlinearly generated daughter Alfvén wave will increase and decrease in time.

C. Nonlinear interactions

The Fourier decomposition of the distorting Alfvén wave above can be used to split the total nonlinear interaction between the probe Alfvén wave and the distorting Alfvén wave into the sum of the interactions between the probe Alfvén wave and each Fourier component of the distorting Alfvén wave. Let us consider each of these interactions in turn, beginning with the energetically dominant components of the distorting Alfvén wave with $k_\parallel = 0$ and $k_\parallel = \pi/L$, as shown in Figure 4.

Based on the theoretical considerations discussed in Sec. II, the $k_\parallel = 0$ component of the distorting Alfvén wave will mediate a three-wave interaction to transfer energy secularly from the probe Alfvén wave to a daughter Alfvén wave. This nonlinear interaction is the desired aim of the experimental design, and we determine the properties of the resulting daughter Alfvén wave in Sec. III D.

The other energetically dominant component of the distorting Alfvén wave, with $k_\parallel = \pi/L$, leads, on the other hand, to no net nonlinear energy transfer due to the three-wave interaction occurring as the probe wave traverses the interaction region. A secular energy transfer can occur due to a four-wave interaction, as explained in Sec. II D, but such an effect is probably not measurable in the laboratory due to the significantly smaller amplitude of any mode generated by a four-wave interaction.

As it turns out, all of the higher wavenumber components (with $k_\parallel > \pi/L$) of the distorting Alfvén wave will likewise lead to zero net energy transfer due to three-wave interactions. This is most easily understood in terms of the magnetic shear associated with each of these modes, as described in Paper V. In general, the three-wave interaction will not produce any net nonlinear energy transfer if the integral of the magnetic fluctuation δB_x over the length $z = 2L$ is zero, as is the case for all of these modes, easily verified by inspection of Figure 4. Paper V demonstrates this point using numerical simulations of collisions between counterpropagating Alfvén wave packets.

In conclusion, only the $k_\parallel = 0$ component of the distorting Alfvén wave, as experienced by the counterpropagating probe Alfvén wave over the length of the interaction region, will lead to a secular transfer of energy from the probe Alfvén wave to a daughter Alfvén wave. This is consistent with findings of Ng and Bhattacharjee[40] that a nonzero $k_\parallel = 0$ component of an Alfvén wavepacket is required to yield nonzero nonlinear energy transfer via a resonant three-wave interaction.

D. Predicted properties of the daughter wave

Let us now predict the properties of the nonlinearly generated daughter Alfvén wave arising from experimental design described here. As we have shown in Sec. III C, only the $k_\parallel = 0$ component of the distorting Alfvén wave leads to a measurable transfer of energy from the probe Alfvén wave to a propagating daughter Alfvén through a resonant three-wave interaction.

First, let us define the wavevectors of the plane-wave Fourier modes associated with each of the interacting, counterpropagating Alfvén wave components. The probe Alfvén wave is launched by the ASW antenna down the magnetic field in the $-\hat{\mathbf{z}}$ direction with the perpendicular waveform shown in panel (b) of Figure 2 in Paper IV. The perpendicular spatial variation of this waveform is almost entirely in the $\hat{\mathbf{x}}$ direction. Therefore, we denote the wavevector of the probe ASW Alfvén wave $\mathbf{z}^+$ by $\mathbf{k}_1 = k_{\perp 1}\hat{\mathbf{x}} + k_{\parallel 1}\hat{\mathbf{z}}$, where $k_{\parallel 1} < 0$ indicates that the wave propagates anti-parallel to the axial magnetic field shown in Figure 2.

Although the distorting Alfvén wave $\mathbf{z}^-$ launched by the Loop antenna has a more complicated perpendicular

waveform, as shown in panel (b) of Figure 3 in Paper IV, we focus on the variation of the δB_x component of the wave magnetic field. In Eq. (1), the vector form of the nonlinear term, $\mathbf{z}^- \cdot \nabla \mathbf{z}^+$, indicates that it is the δB_x component of the distorting Alfvén wave $\mathbf{z}^-$ that will interact nonlinearly with the probe Alfvén wave $\mathbf{z}^+$; this follows because the perpendicular component of the wavevector $\mathbf{k}_1$ of the probe Alfvén wave is in the $\hat{\mathbf{x}}$-direction. As shown in panel (b) of Figure 7 in Paper IV, the perpendicular Fourier transform of the δB_x component of the distorting Loop Alfvén wave has very little power with $k_x \neq 0$, so the wavevector is dominantly in the y-direction. Only the component with $k_{\|2} = 0$ of the distorting Loop Alfvén wave leads to a net nonlinear energy transfer through the three-wave interaction, so the wavevector of the relevant Fourier mode for the distorting Alfvén wave is given by $\mathbf{k}_2 = k_{\perp 2}\hat{\mathbf{y}}$. For simplicity in the discussion below, when we refer to distorting Alfvén wave, we specifically consider *only* this Fourier component $\mathbf{k}_2$ of that wave, since the other components lead to zero net energy transfer via three-wave interactions.

The wavevector of the daughter Alfvén wave resulting from the nonlinear interaction between the distorting and probe Alfvén waves in the experiment is denoted by $\mathbf{k}_3 = \mathbf{k}_{\perp 3} + k_{\|3}\hat{\mathbf{z}}$. The resonance conditions for the three-wave interactions given by Eq. (4) enable us to predict $\mathbf{k}_{\perp 3}$ and $k_{\|3}$ in terms of $k_{\perp 1}$, $k_{\|1}$, $k_{\perp 2}$, and $k_{\|2}$.

Before applying the resonance conditions Eq. (4), we need to determine the frequency ω_2 associated with the Fourier mode $\mathbf{k}_2$ of the distorting Alfvén wave. As illustrated by panel (b) of Figure 4, the perpendicular magnetic field fluctuation δB_x associated with the $k_{\|2} = 0$ component of the distorting Alfvén wave is constant as experienced by any single point on the counterpropagating probe Alfvén wave. Therefore, this component will have zero frequency, $\omega_2 = 0$, from the perspective of the counterpropagating wave. The probe Alfvén wave launched by the ASW antenna is a linear Alfvén wave, so its frequency is given by the linear dispersion relation, $\omega_1 = |k_{\|1}| v_A$, where we reiterate that $k_{\|1} < 0$ to denote that the probe Alfvén wave travels down the axial magnetic field in the experiment.

Now that we have specified the wavevectors and frequencies of the distorting and probe Alfvén waves that lead to energy transfer via a resonant three-wave interaction, we can compute the properties of the nonlinearly generated daughter Alfvén wave. The resonance conditions Eq. (4) simplify to the following two equations:

$$\mathbf{k}_{\perp 1} + \mathbf{k}_{\perp 2} = \mathbf{k}_{\perp 3}, \tag{5}$$

$$k_{\|1} = k_{\|3}. \tag{6}$$

We now discuss the implications of these properties for the measurement of the daughter Alfvén wave in the laboratory.

The first distinguishing feature of the daughter Alfvén wave is that its perpendicular wavevector is the vector sum of the perpendicular wavevectors of distorting and probe Alfvén waves, $\mathbf{k}_{\perp 3} = \mathbf{k}_{\perp 1} + \mathbf{k}_{\perp 2}$. Fourier transformation of the measured fluctuations over the perpendicular plane enables a clean separation of the daughter Alfvén wave signal from its parent Alfvén waves, as shown in panel (a) of Figure 7 in Paper IV.

A second technique for isolating the daughter wave signal is to exploit the constraint from Maxwell's equations that the magnetic field fluctuations associated with Alfvén waves must be divergence free, $\nabla \cdot \delta \mathbf{B} = 0$. In the MHD limit relevant to the proposed experiment, $k_\perp \rho_s \ll 1$, where ρ_s is the ion sound Larmor radius, the Alfvén wave eigenfunction has a negligible parallel magnetic field fluctuation, $\delta B_\| = 0$. Therefore, the divergence-free condition for a particular plane wave mode reduces to $\mathbf{k}_\perp \cdot \delta \mathbf{B}_\perp = 0$. This means that the magnetic field fluctuation associated with a plane Alfvén wave is orthogonal to the perpendicular component of the wavevector. This property suggests a simple way to separate the signal of the daughter Alfvén wave from the probe Alfvén wave. The perpendicular wavevector of the probe Alfvén wave is $\mathbf{k}_{\perp 1} = k_{\perp 1}\hat{\mathbf{x}}$, so this divergence-free property dictates that the probe Alfvén wave has $\delta B_{x1} = 0$. The daughter Alfvén wave, on the other hand, has $\mathbf{k}_{\perp 3} = k_{\perp 1}\hat{\mathbf{x}} + k_{\perp 2}\hat{\mathbf{y}}$, so its magnetic field fluctuation is polarized in the direction $\hat{\mathbf{z}} \times \hat{\mathbf{k}}_{\perp 3} = (k_{\perp 1}/k_{\perp 3})\hat{\mathbf{y}} - (k_{\perp 2}/k_{\perp 3})\hat{\mathbf{x}}$, where $k_{\perp 3} = \sqrt{k_{\perp 1}^2 + k_{\perp 2}^2}$. The relation between the components of $\delta \mathbf{B}_3$ is $\delta B_{x3} = -(k_{\perp 2}/k_{\perp 1})\delta B_{y3}$. Therefore, by measuring the δB_x component of the wave magnetic fields in the experiment, the daughter Alfvén wave can be measured without interference from the signal of the probe Alfvén wave.

A third property of the daughter Alfvén wave follows from the parallel component of its wavevector, $k_{\|3} = k_{\|1}$. Since the sign of $k_\|$ indicates the propagation direction, this implies that the daughter Alfvén wave propagates in the same direction as the probe Alfvén wave. This also implies that there is no parallel cascade of energy, consistent with the expectations from weak turbulence theory[11,25,40,43] and the asymptotic analytical solution derived in Paper I.

Following from $k_{\|3} = k_{\|1}$ and the linear dispersion relation for Alfvén waves, $\omega = |k_\||v_A$, a fourth distinguishing feature of the daughter Alfvén wave is that it has the same frequency as the probe Alfvén wave, $\omega_3 = \omega_1$. Since the experimental design outlined in this paper employs a much lower frequency distorting Alfvén wave launched by the Loop antenna (considering here the full signal of this wave, not just the $k_{\|2} = 0$ Fourier component), $\omega_2 < \omega_1$, this enables the daughter Alfvén wave signal to be separated from the distorting Alfvén wave by filtering in frequency.

The asymptotic analytical solution derived in Paper I suggests additional distinguishing features of the daughter Alfvén wave. A fifth property is that any daughter Alfvén wave receiving a secular transfer of energy from a parent Alfvén wave should have a $\pi/2$ phase shift with respect to the parent wave, as indicated by the solution for the secularly increasing mode in Eq. (40) of Paper I. This prediction is supported by the numerical simulations presented in Paper V.

A sixth property of the daughter Alfvén wave, suggested by the analytical solution, is the predicted amplitude of the signal. Although the analytical solution derived in Paper I is computed for a symmetric case of perpendicularly polarized, counterpropagating Alfvén waves with the same magnitude of $k_\perp$ and equal and opposite values of $k_\|$, the solution

nonetheless should provide a reasonable order-of-magnitude or better estimate of the amplitude of the signal generated by nonlinear three-wave interactions. The coefficient of the magnetic field perturbation due to the lowest-order nonlinear solution, given by Eq. (36) in Paper I, is

$$\frac{|\mathbf{B}_{\perp 2}|}{B_0} \sim \frac{z_+ z_-}{16 v_A^2} \frac{k_\perp}{k_\parallel}, \tag{7}$$

where $z_\pm/v_A$ represents the normalized amplitude of the Elsasser fields $\mathbf{z}^\pm$ associated with the primary counterpropagating Alfvén waves. Using the linear eigenfunction for Alfvén waves, $\mathbf{u}_\perp/v_A = \pm \delta \mathbf{B}_\perp/B_0$, we can relate the Elsasser field amplitude to the perturbed magnetic field amplitude, $|\mathbf{z}^\pm|/v_A = 2|\mathbf{B}_\perp|/B_0$. Therefore, the relation for the amplitude of the daughter wave $\delta B_{\perp 3}$ can be simplified to

$$\frac{\delta B_{\perp 3}}{B_0} \sim \frac{1}{4} \frac{\delta B_{\perp 1}}{B_0} \frac{\delta B_{\perp 2}}{B_0} \frac{k_{\perp 1}}{k_{\parallel 1}}, \tag{8}$$

where the $k_{\perp 1}$ and $k_{\parallel 1}$ are the wavevector components of the probe Alfvén wave, $\delta B_{\perp 1}$ is the amplitude of the probe Alfvén wave, and $\delta B_{\perp 2}$ corresponds to the amplitude of only the $k_{\parallel 2} = 0$ component of the distorting Alfvén wave. This amplitude prediction can be used to determine whether the measured daughter Alfvén wave signal is consistent with theoretical expectations.

A final qualitative characteristic of the daughter Alfvén wave signal arises because the coefficient of the $k_{\parallel 2} = 0$ component of the distorting Alfvén wave oscillates in time, as mentioned in the final paragraph of Sec. III B. Since the amplitude of the $k_{\parallel 2} = 0$ component varies depending on the section of the distorting Alfvén wave that interacts with the probe Alfvén wave over the interaction region, the net nonlinear energy transfer to the daughter Alfvén wave oscillates with the amplitude of the $k_{\parallel 2} = 0$ component. This $k_{\parallel 2} = 0$ amplitude oscillates at the frequency of the distorting Alfvén wave, so we expect that amplitude of the nonlinear daughter wave signal will increase and decrease at distorting Alfvén wave frequency.

E. Relation to recent laboratory experiments

It is worth highlighting here the contrasts between the present experimental investigation of Alfvén wave collisions as the fundamental building block of plasma turbulence and a recent experimental study exploring the physics of the parametric decay instability using the nonlinear interaction between counterpropagating Alfvén waves by Dorfman and Carter.[49]

It has long been known that finite-amplitude Alfvén waves are nonlinearly unstable to parametric instabilities driven by gradients parallel to the magnetic field, including the decay,[50,51] modulational,[52] and beat[53,54] instabilities. In particular, the parametric decay instability involves the nonlinear decay of a large-amplitude Alfvén wave into an ion acoustic wave propagating in the same direction and an Alfvén wave propagating in the opposite direction.[51] Thus, the parametric decay instability relies on a nonlinear mode coupling between Alfvén and ion acoustic waves. Dorfman and Carter[49] performed the first laboratory measurements of a related Alfvén-acoustic mode coupling in which two counterpropagating Alfvén waves interact nonlinearly to generate resonantly an ion acoustic mode at the resulting beat frequency.

Although the experimental setup on the Large Plasma Device (LAPD) at UCLA for the Dorfman and Carter study involved the nonlinear interaction between counterpropagating Alfvén waves—and may therefore appear very similar to the present study—the two investigations, in fact, probe entirely distinct nonlinear physical mechanisms. Our study probes the nonlinearity associated with the perpendicular gradients of the wave magnetic fields, generically labeled the $\mathbf{E} \times \mathbf{B}$ nonlinearity in Paper I,[16] whereas the Dorfman and Carter study explores the nonlinear ponderomotive force due to parallel gradients of the magnetic field magnitude. The $\mathbf{E} \times \mathbf{B}$ nonlinearity operates in an incompressible plasma but requires that the counterpropagating Alfvén waves have wavevectors $\mathbf{k}^+$ and $\mathbf{k}^-$ with nonzero perpendicular components that are not collinear, $\mathbf{k}_\perp^+ \times \mathbf{k}_\perp^- \neq 0$. Simply put, the $\mathbf{E} \times \mathbf{B}$ nonlinearity occurs between counterpropagating, perpendicularly polarized Alfvén waves. In contrast, the physics of the parametric decay instability explored by Dorfman and Carter requires compressibility but does not demand that either Alfvén wave have perpendicular spatial variation, occurring even when $\mathbf{k}_\perp^+ = \mathbf{k}_\perp^- = 0$. The wave magnetic fields, on the other hand, cannot be perpendicularly polarized, so that $\delta \mathbf{B}_\perp^+ \cdot \delta \mathbf{B}_\perp^- \neq 0$. Simply put, the nonlinearity studied by Dorfman and Carter occurs between counterpropagating Alfvén waves polarized in the same direction. It is clear that these two experiments have been designed specifically to probe distinct nonlinear mechanisms.

A number of studies have suggested that the nonlinearities associated with the decay instability or other parametric instabilities play a role in the nonlinear evolution of turbulence in the solar wind or other astrophysical plasmas.[53–61] However, the majority of the literature on parametric instabilities adopts the oft-assumed "slab" geometry, a one-dimensional treatment in which the waves vary only parallel to the magnetic field, so $k_\perp = 0$ for all modes. This limitation eliminates the possibility of the $\mathbf{E} \times \mathbf{B}$ nonlinearity, a nonlinearity that will dominate under conditions in which the turbulent fluctuations are highly elongated along the local mean magnetic field, $k_\perp \gg k_\parallel$, a property strongly supported by recent multi-spacecraft observations of turbulence in the solar wind.[30,31,62] In the introduction to Paper I,[16] we propose the working hypothesis that the $\mathbf{E} \times \mathbf{B}$ nonlinearity is the dominant nonlinear mechanism underlying the anisotropic cascade of energy in magnetized plasma turbulence, and there we present a detailed argument in support of this hypothesis. Briefly, the argument is that nonlinearities associated with parallel gradients, such as the parametric instabilities, contribute significantly to the nonlinear evolution only for finite amplitude fluctuations, $\delta v/v_A \sim 1$; on the other hand, the $\mathbf{E} \times \mathbf{B}$ nonlinearity depends on the perpendicular gradients, and can therefore contribute significantly even if $\delta v/v_A \ll 1$, as long as the turbulent fluctuations are significantly anisotropic, $k_\perp/k_\parallel \gg 1$. Furthermore, that a nonlinear

mechanism involving compressibility is not required by Alfvénic plasma turbulence is supported by the fact that both incompressible[26,27] and compressible[63] MHD turbulence simulations recover quantitatively similar turbulent energy spectra for the Alfvénic fluctuations.

IV. CONCLUSION

In this paper, we describe the theoretical background of Alfvén wave collisions used to design an experiment to measure in the laboratory for the first time the nonlinear interaction between counterpropagating Alfvén waves. This successful measurement has established a firm basis for the application of theoretical ideas developed in idealized models to turbulence in realistic space and astrophysical plasma systems.[15] The theoretical considerations here and the details of the experimental procedure and analysis in a companion work by Drake *et al.*,[18] (Paper IV) provide the necessary background for this experimental effort.

The experiment is designed to measure the propagating daughter Alfvén wave generated by the nonlinear interaction between perpendicularly polarized, counterpropagating Alfvén waves. This nonlinear interaction is the fundamental building block of astrophysical plasma turbulence. In order to generate a measurable signal in the experiment, a relatively large-amplitude, low-frequency Alfvén wave is employed to distort nonlinearly a counterpropagating, smaller-amplitude, higher-frequency Alfvén wave. The parallel wavelength of the low-frequency Alfvén wave exceeds twice the length of the experimental interaction region, generating an effective $k_\parallel = 0$ component that is experienced by the counterpropagating high-frequency Alfvén wave. This $k_\parallel = 0$ component mediates a resonant three-wave interaction that transfers energy secularly from initial high-frequency Alfvén wave to a nonlinearly generated daughter Alfvén wave.

For the three-wave interaction in the experiment between a high-frequency Alfvén wave with wavevector $\mathbf{k}_1 = k_{\perp 1}\hat{\mathbf{x}} + k_{\parallel 1}\hat{\mathbf{z}}$ and a counterpropagating low-frequency Alfvén wave with a $k_{\parallel 2} = 0$ component with wavevector $\mathbf{k}_2 = k_{\perp 2}\hat{\mathbf{y}}$, we expect nonlinear energy transfer to a propagating daughter Alfvén wave with wavevector $\mathbf{k}_3 = \mathbf{k}_{\perp 3} + k_{\parallel 3}\hat{\mathbf{z}}$. We predict the following properties of the daughter Alfvén wave based on the theoretical considerations outlined in this paper:

1. Perpendicular wavevector: $\mathbf{k}_{\perp 3} = \mathbf{k}_{\perp 1} + \mathbf{k}_{\perp 2}$.
2. Propagation direction: $k_{\parallel 3} = k_{\parallel 1}$.
3. Frequency: $\omega_3 = \omega_1$.
4. Magnetic field: $\delta B_{x3} = -(k_{\perp 2}/k_{\perp 1})\delta B_{y3}$.
5. Phase: Daughter Alfvén wave phase-shifted by $\pi/2$ from the probe Alfvén wave.
6. Amplitude: $\delta B_{\perp 3}/B_0 \sim (1/4)(\delta B_{\perp 1}/B_0)(\delta B_{\perp 2}/B_0)(k_{\perp 1}/k_{\parallel 1})$.

These theoretically predicted properties of the daughter Alfvén wave can be used to demonstrate conclusively that our experiment[15] has indeed lead to the first successful measurement of an Alfvén wave generated by the nonlinear interaction between counterpropagating Alfvén waves, as detailed in Paper IV.

A critical point of this analysis is that any localized Alfvén wavepacket with an asymmetric waveform carries a $k_\parallel = 0$ component. This $k_\parallel = 0$ component can lead to the secular transfer of energy to Alfvén waves with higher perpendicular wavenumber through resonant three-wave interactions. Since Alfvén wavepackets in weakly turbulent astrophysical plasmas will not generally have symmetric waveforms, three-wave interactions are expected to dominate the nonlinear energy transfer. The experimental design described here has successfully demonstrated in the laboratory[15] the nonlinear energy transfer by resonant three-wave interactions in a weakly turbulent plasma system in the MHD regime.

In a forthcoming work (Paper V[19]), nonlinear gyrokinetic simulations of the interaction between localized, counterpropagating Alfvén wavepackets will be used to illustrate this concept of energy transfer by resonant three-wave interactions when asymmetric Alfvén waveforms collide. Furthermore, the $k_\parallel = 0$ component of an Alfvén wavepacket will be interpreted physically as a finite magnetic shear, establishing a firm connection between the concepts of magnetic field line wander and turbulence in astrophysical plasmas.

ACKNOWLEDGMENTS

This work was supported by NSF PHY-10033446, NSF CAREER AGS-1054061, NSF CAREER PHY-0547572, and NASA NNX10AC91G. This works describes the design of an experiment conducted at the Basic Plasma Science Facility, funded by the U.S. Department of Energy and the National Science Foundation.

[1]S. W. McIntosh, B. de Pontieu, M. Carlsson, V. Hansteen, P. Boerner, and M. Goossens, "Alfvénic waves with sufficient energy to power the quiet solar corona and fast solar wind," Nature **475**, 477–480 (2011).
[2]J. W. Armstrong, J. M. Cordes, and B. J. Rickett, "Density power spectrum in the local interstellar medium," Nature **291**, 561–564 (1981).
[3]J. W. Armstrong, B. J. Rickett, and S. R. Spangler, "Electron density power spectrum in the local interstellar medium," Astrophys. J. **443**, 209–221 (1995).
[4]B. M. Gaensler, M. Haverkorn, B. Burkhart, K. J. Newton-McGee, R. D. Ekers, A. Lazarian, N. M. McClure-Griffiths, T. Robishaw, J. M. Dickey, and A. J. Green, "Low-Mach-number turbulence in interstellar gas revealed by radio polarization gradients," Nature **478**, 214–217 (2011); e-print arXiv:1110.2896 [astro-ph.GA].
[5]B. J. Rickett, "Radio propagation through the turbulent interstellar plasma," Ann. Rev. Astron. Astrophys. **28**, 561–605 (1990).
[6]J. R. Peterson and A. C. Fabian, "X-ray spectroscopy of cooling clusters," Phys. Rep. **427**, 1–39 (2006); e-print arXiv:astro-ph/0512549.
[7]D. Sundkvist, V. Krasnoselskikh, P. K. Shukla, A. Vaivads, M. André, S. Buchert, and H. Rème, "In situ multi-satellite detection of coherent vortices as a manifestation of Alfvénic turbulence," Nature **436**, 825–828 (2005).
[8]H. Alfvén, "Existence of electromagnetic-hydrodynamic waves," Nature **150**, 405–406 (1942).
[9]J. W. Belcher and L. Davis, "Large-amplitude Alfvén waves in the interplanetary medium, 2," J. Geophys. Res. **76**, 3534–3563, doi:10.1029/JA076i016p03534 (1971).
[10]R. H. Kraichnan, "Inertial range spectrum of hyromagnetic turbulence," Phys. Fluids **8**, 1385–1387 (1965).
[11]S. Sridhar and P. Goldreich, "Toward a theory of interstellar turbulence. 1: Weak Alfvenic turbulence," Astrophys. J. **432**, 612–621 (1994).

[12]P. Goldreich and S. Sridhar, "Toward a theery of interstellar turbulence ii. Strong Alfvénic turbulence," Astrophys. J. **438**, 763–775 (1995).
[13]S. Boldyrev, "Spectrum of magnetohydrodynamic turbulence," Phys. Rev. Lett. **96**, 115002 (2006); e-print arXiv:astro-ph/0511290.
[14]W. Gekelman, H. Pfister, Z. Lucky, J. Bamber, D. Leneman, and J. Maggs, "Design, construction, and properties of the large plasma research device—The LAPD at UCLA," Rev. Sci. Instrum. **62**, 2875–2883 (1991).
[15]G. G. Howes, D. J. Drake, K. D. Nielson, T. A. Carter, C. A. Kletzing, and F. Skiff, "Toward astrophysical turbulence in the laboratory," Phys. Rev. Lett. **109**, 255001 (2012); e-print arXiv:1210.4568 [physics.plasm-ph].
[16]G. G. Howes and K. D. Nielson, "Alfven wave collisions, the fundamental building block of plasma turbulence. I. Asymptotic solution," Phys. Plasmas **20**, 072302 (2013).
[17]K. D. Nielson, G. G. Howes, and W. Dorland, "Alfven wave collisions, the fundamental building block of plasma turbulence. II. Numerical solution," Phys. Plasmas **20**, 072303 (2013).
[18]D. J. Drake, J. W. R. Schroeder, G. G. Howes, F. Skiff, C. A. Kletzing, T. A. Carter, and D. W. Auerbach, "Alfven wave collisions, the fundamental building block of plasma turbulence. IV. Laboratory experiment," Phys. Plasmas **20**, 072901 (2013).
[19]G. G. Howes, K. D. Nielson, J. W. R. Schroeder, D. J. Drake, F. Skiff, C. A. Kletzing, and T. A. Carter, "Alfven wave collisions, the fundamental building block of plasma turbulence V: Simulations and magnetic shear interpretation," Phys. Plasmas (to be published).
[20]W. M. Elsasser, "The hydromagnetic equations," Phys. Rev. **79**, 183 (1950).
[21]A. A. Schekochihin, S. C. Cowley, W. Dorland, G. W. Hammett, G. G. Howes, E. Quataert, and T. Tatsuno, "Astrophysical gyrokinetics: Kinetic and fluid turbulent cascades in magnetized weakly collisional plasmas," Astrophys. J. Supp. **182**, 310–377 (2009).
[22]D. C. Robinson and M. G. Rusbridge, "Structure of turbulence in the zeta plasma," Phys. Fluids **14**, 2499–2511 (1971).
[23]S. J. Zweben, C. R. Menyuk, and R. J. Taylor, "Small-scale magnetic fluctuations inside the macrotor tokamak," Phys. Rev. Lett. **42**, 1270–1274 (1979).
[24]D. Montgomery and L. Turner, "Anisotropic magnetohydrodynamic turbulence in a strong external magnetic field," Phys. Fluids **24**, 825–831 (1981).
[25]J. V. Shebalin, W. H. Matthaeus, and D. Montgomery, "Anisotropy in MHD turbulence due to a mean magnetic field," J. Plasma Phys. **29**, 525–547 (1983).
[26]J. Cho and E. T. Vishniac, "The anisotropy of magnetohydrodynamic Alfvénic turbulence," Astrophys. J. **539**, 273–282 (2000).
[27]J. Maron and P. Goldreich, "Simulations of incompressible magnetohydrodynamic turbulence," Astrophys. J. **554**, 1175–1196 (2001).
[28]J. Cho and A. Lazarian, "The Anisotropy of Electron Magnetohydrodynamic Turbulence," Astrophys. J. Lett. **615**, L41–L44 (2004).
[29]J. Cho and A. Lazarian, "Simulations of electron magnetohydrodynamic turbulence," Astrophys. J. **701**, 236–252 (2009); e-print arXiv:0904.0661 [astro-ph.EP].
[30]F. Sahraoui, M. L. Goldstein, G. Belmont, P. Canu, and L. Rezeau, "Three dimensional anisotropic k spectra of turbulence at subproton scales in the solar wind," Phys. Rev. Lett. **105**, 131101 (2010).
[31]Y. Narita, S. P. Gary, S. Saito, K.-H. Glassmeier, and U. Motschmann, "Dispersion relation analysis of solar wind turbulence," Geophys. Res. Lett. **38**, L05101, 10.1029/2010GL046588 (2011).
[32]J. M. TenBarge and G. G. Howes, "Evidence of critical balance in kinetic Alfvén wave turbulence simulations," Phys. Plasmas **19**, 055901 (2012).
[33]P. S. Iroshnikov, "The turbulence of a conducting fluid in a strong magnetic field," Astron. Zh. **40**, 742 (1963) [Sov. Astron. **7**, 566 (1964)].
[34]Y. Lithwick, P. Goldreich, and S. Sridhar, "Imbalanced strong MHD turbulence," Astrophys. J. **655**, 269–274 (2007); e-print arXiv:astro-ph/0607243.
[35]A. Beresnyak and A. Lazarian, "Strong imbalanced turbulence," Astrophys. J. **682**, 1070–1075 (2008); e-print arXiv:0709.0554.
[36]B. D. G. Chandran, "Strong anisotropic MHD turbulence with cross helicity," Astrophys. J. **685**, 646–658 (2008); e-print arXiv:0801.4903.
[37]J. C. Perez and S. Boldyrev, "Role of cross-helicity in magnetohydrodynamic turbulence," Phys. Rev. Lett. **102**, 025003 (2009); e-print arXiv:0807.2635.
[38]J. J. Podesta and A. Bhattacharjee, "Theory of incompressible magnetohydrodynamic turbulence with scale-dependent alignment and cross-helicity," Astrophys. J. **718**, 1151–1157 (2010); e-print arXiv:0903.5041 [astro-ph.EP].
[39]S. Galtier, S. V. Nazarenko, A. C. Newell, and A. Pouquet, "A weak turbulence theory for incompressible magnetohydrodynamics," J. Plasma Phys. **63**, 447–488 (2000).
[40]C. S. Ng and A. Bhattacharjee, "Interaction of shear-Alfven wave packets: Implication for weak magnetohydrodynamic turbulence in astrophysical plasmas," Astrophys. J. **465**, 845 (1996).
[41]Y. Lithwick and P. Goldreich, "Imbalanced weak magnetohydrodynamic turbulence," Astrophys. J. **582**, 1220–1240 (2003).
[42]D. Montgomery and W. H. Matthaeus, "Anisotropic modal energy transfer in interstellar turbulence," Astrophys. J. **447**, 706 (1995).
[43]P. Goldreich and S. Sridhar, "Magnetohydrodynamic turbulence revisited," Astrophys. J. **485**, 680–688 (1997).
[44]D. W. Auerbach, T. A. Carter, S. Vincena, and P. Popovich, "Resonant drive and nonlinear suppression of gradient-driven instabilities via interaction with shear Alfvén waves," Phys. Plasmas **18**, 055708 (2011).
[45]D. J. Thuecks, C. A. Kletzing, F. Skiff, S. R. Bounds, and S. Vincena, "Tests of collision operators using laboratory measurements of shear Alfvén wave dispersion and damping," Phys. Plasmas **16**, 052110 (2009).
[46]C. A. Kletzing, D. J. Thuecks, F. Skiff, S. R. Bounds, and S. Vincena, "Measurements of inertial limit Alfvén wave dispersion for finite perpendicular wave number," Phys. Rev. Lett. **104**, 095001 (2010).
[47]K. D. Nielson, G. G. Howes, T. Tatsuno, R. Numata, and W. Dorland, "Numerical modeling of large plasma device Alfvén wave experiments using AstroGK," Phys. Plasmas **17**, 022105 (2010).
[48]D. J. Drake, C. A. Kletzing, F. Skiff, G. G. Howes, and S. Vincena, "Design and use of an Elsässer probe for analysis of Alfvén wave fields according to wave direction," Rev. Sci. Instrum. **82**, 103505 (2011).
[49]S. Dorfman and T. A. Carter, "Nonlinear excitation of acoustic modes by large-amplitude Alfvén waves in a laboratory plasma," Phys. Rev. Lett. **110**, 195001 (2013); e-print arXiv:1304.3379 [physics.plasm-ph].
[50]A. A. Galeev and V. N. Oraevskii, "The stability of Alfvén waves," Sov. Phys. Dokl. **7**, 988 (1963).
[51]R. Z. Sagdeev and A. A. Galeev, *Nonlinear Plasma Theory* (New York, Benjamin, 1969).
[52]C. N. Lashmore-Davies, "Modulational instability of a finite amplitude Alfven wave," Phys. Fluids **19**, 587–589 (1976).
[53]H. K. Wong and M. L. Goldstein, "Parametric instabilities of the circularly polarized Alfven waves including dispersion," J. Geophys. Res. **91**, 5617–5628, doi:10.1029/JA091iA05p05617 (1986).
[54]J. V. Hollweg, "Beat, modulational, and decay instabilities of a circularly polarized Alfven wave," J. Geophys. Res. **99**, 23431, doi:10.1029/94JA02185 (1994).
[55]N. F. Derby, Jr., "Modulational instability of finite-amplitude, circularly polarized Alfven waves," Astrophys. J. **224**, 1013–1016 (1978).
[56]M. L. Goldstein, "An instability of finite amplitude circularly polarized Alfven waves," Astrophys. J. **219**, 700–704 (1978).
[57]S. R. Spangler and J. P. Sheerin, "Properties of Alfven solitons in a finite-beta plasma," J. Plasma Phys. **27**, 193–198 (1982).
[58]J.-I. Sakai and U. O. Sonnerup, "Modulational instability of finite amplitude dispersive Alfven waves," J. Geophys. Res. **88**, 9069–9079, doi:10.1029/JA088iA11p09069 (1983).
[59]S. R. Spangler, "The evolution of nonlinear Alfven waves subject to growth and damping," Phys. Fluids **29**, 2535–2547 (1986).
[60]T. Terasawa, M. Hoshino, J.-I. Sakai, and T. Hada, "Decay instability of finite-amplitude circularly polarized Alfven waves—A numerical simulation of stimulated Brillouin scattering," J. Geophys. Res. **91**, 4171–4187, doi:10.1029/JA091iA04p04171 (1986).
[61]V. I. Shevchenko, R. Z. Sagdeev, V. L. Galinsky, and M. V. Medvedev, "The DNLS equation and parametric decay instability," Plasma Phys. Rep. **29**, 545–549 (2003).
[62]O. W. Roberts, X. Li, and B. Li, "Kinetic plasma turbulence in the fast solar wind measured by Cluster," Astrophys. J. **769**, 58 (2013); e-print arXiv:1303.5129 [astro-ph.SR].
[63]J. Cho and A. Lazarian, "Compressible magnetohydrodynamic turbulence:Mode coupling, scaling relations, anisotropy, viscosity-damped regime and astrophysical implications," Mon. Not. Roy. Astron. Soc. **345**, 325–339 (2003).